EFFECTS OF LONG RANGE ORDERING, TEMPERATURE AND STRAIN RATE ON DEFORMATION BEHAVIOR OF A Ni-Mo-Cr ALLOY

S. Dymek*[1], M. Dollar*, A. Iyer* and D.L. Klarstrom@

*Illinois Institute of Technology, Chicago, Il. 60616
@Haynes® International, Inc., Kokomo, In. 46902

Abstract

Deformation mechanisms and tensile properties in a high-temperature, Ni-Mo-Cr, aged-hardenable alloy, HAYNES® 242™ alloy, strengthened by extremely small ordered particles were investigated at different temperatures and strain rates. The unaged specimens deformed predominantly by crystallographic slip. In the aged specimens, microtwinning was found to be a predominant deformation mechanism. This change of deformation mode is attributed to the presence of the ordered particles which constitute effective dislocation barriers and restrict cross-slip. Serrations in the stress-strain curves were observed in the unaged and aged specimens deformed at elevated temperatures. The occurrence of the jerky flow coincided with the negative value of strain rate sensitivity, implying a role of dynamic strain aging. The jerky flow was delayed to higher strains and temperatures in the aged specimens, an effect which is believed to shed light on the origins of the jerky flow in the presence of ordered particles.

® HAYNES and 242 are trademarks of Haynes International, Inc.

[1]On leave from Academy of Mining and Metallurgy, Kraków, Poland.

Superalloys 1992
Edited by S.D. Antolovich, R.W. Stusrud, R.A. MacKay,
D.L. Anton, T. Khan, R.D. Kissinger, D.L. Klarstrom
The Minerals, Metals & Materials Society, 1992

Introduction

The Ni-Mo-Cr system forms the basis for a number of commercial alloys such as high-temperature HASTELLOY®[2] alloys S, N, B (1), and corrosion resistant HASTELLOY alloys C-4, C-276 (2). Recently, another high-temperature Ni-Mo-Cr alloy, HAYNES® 242™ alloy, has been developed (1,3,4). This age-hardenable alloy, consisting essentially of Ni—25%Mo—8%Cr, utilizes a long-range-ordering reaction to form uniformly sized and distributed, extremely small (about 10nm), ordered particles. The alloy exhibits excellent strength and ductility at elevated temperatures, low thermal expansion characteristics and good oxidation resistance (1).

The present research has been undertaken to explore deformation mechanisms and to examine tensile properties in unaged and aged 242 alloy tested at ambient and elevated temperatures and at different strain rates.

Experimental Procedure

The chemical composition of the material used in the present study, 242 alloy is given in Table I. The alloy was solution heat treated at 1065°C, quenched and subsequently aged for 24 hours at different temperatures. All heat treatments were carried out on previously machined tensile specimens (gauge length 25.4mm, diameter 4.1mm) encapsulated in quartz.

Table I. Chemical composition [wt.%]

Ni	Mo	Cr	C
Bal	25.13	7.82	0.01

Tensile tests of unaged as well as aged specimens were conducted on an INSTRON machine at three different strain rates: $\dot{\epsilon}_1=8\text{x}10^{-4}$, $\dot{\epsilon}_2=8\text{x}10^{-3}$ and $\dot{\epsilon}_3=8\text{x}10^{-2}$, at room and elevated temperatures. Elevated temperature tests were carried out in a closed cell furnace in air. The strain hardening exponent, **n**, was calculated using Ludwik equation:

$$\ln(\sigma-\sigma_0)=k+n\ln\epsilon$$

Strain rate change tests were also conducted. Strain rate changes $\dot{\epsilon}_2/\dot{\epsilon}_1=10$ were used to measure strain rate sensitivity (5,6):

$$\beta\equiv\frac{\Delta\sigma}{\Delta\ln\dot{\epsilon}}$$

True stresses and strains were used in the above equations.

Transmission electron microscopy (TEM) was carried out on longitudinal sections of the tensile specimens. Discs for TEM were electrolytically thinned by a jet technique, using a solution of 1 part HNO_3 and 3 parts methanol (U=30V, temp. ≈ -30°C). Thin foils were examined at 100kV in a JEOL 100CX microscope. Investigation of the fracture surfaces was carried out in a JEOL scanning electron microscope (SEM).

Results

Mechanical Properties

The tensile properties of unaged specimens and specimens aged at different temperatures, tested at room temperature and the intermediate strain rate of $\dot{\epsilon}_2=8\text{x}10^{-3}\ s^{-1}$, are shown in Table II. The data confirm that aging at 650°C for 24 hours (the standard procedure for 242 alloy (4)) results in an

[2] ® HASTELLOY is a registered trademark of Haynes International, Inc.

optimum combination of mechanical properties. The yield strength of the material aged at 650°C doubles that of the unaged material, the work hardening is strong, and a relatively high room temperature ductility is maintained. All tests were carried out on specimens subjected to this aging procedure.

Table II. Room temperature tensile properties of unaged and aged specimens ($\dot{\epsilon}_2=8x10^{-3}s^{-1}$).

Aging Temp. °C	YS MPa	UTS MPa	el. %	RA %	n -
unaged	464	995	50	65	0.81
625	678	1236	38	36	0.84
650	952	1418	31	37	0.87
700	813	1397	31	32	0.91
725	765	1338	25	26	0.92
760	448	945	43	49	0.82

el. - elongation to failure
RA - reduction in area

The yield strength and work hardening exponent of the unaged and aged specimens tested at different temperatures and strain rates are shown in Tables III and IV, respectively.

The yield strength of the unaged material decreases between room temperature and 350°C but remains nearly the same at 500°C. The strength retention is addressed in the discussion. The yield strength of the aged material decreases with the increase in the testing temperature, not an unexpected result, and remains relatively high at 650-700°C, the anticipated service temperature range of the 242 alloy. On the other hand, the yield strength tends to decrease with increasing strain rate, an unusual effect to be addressed in the discussion.

At elevated temperatures, serrated yielding (jerky flow) was observed in both the unaged and aged specimens, and the deformation corresponding to the onset of the jerky flow, ϵ_c, is tabulated in Tables III and IV. The critical strain decreased with increasing test temperature, and decreasing strain rate. At the lowest strain rate, the onset of jerky flow and plastic deformation usually coincided. The exemplary stress-strain curves for the aged material, obtained at the strain rate of $\dot{\epsilon}_1=8x10^{-4}s^{-1}$, are shown in Fig.1, illustrating the occurrence and distinctive, depending on temperature, character of serrated yielding. To shed light on the origins of the jerky flow in the present alloy, strain rate change tests were carried out and the strain rate sensitivity, β, was measured. The relationships between the strain rate sensitivity and flow stress, for different temperatures, in the unaged and aged materials are shown in Figs. 2a and 2b, respectively.

Table III. Tensile properties of the unaged material.

strain rate	25°C			350°C			500°C		
	YS MPa	n -	ϵ_c %	YS MPa	n -	ϵ_c %	YP MPa	n -	ϵ_c %
$\dot{\epsilon}_1=8x10^{-4}$	497	.82	-	394	.68	4	385	.74	YP
$\dot{\epsilon}_2=8x10^{-3}$	464	.81	-	352	.76	28	382	.70	7
$\dot{\epsilon}_3=8x10^{-2}$	408	.77	-	343	.59	30	326	.68	13

Table IV. Tensile properties of the aged material (650°C/24h).

Testing temp. °C	$\dot{\epsilon}_1=8x10^{-4}$			$\dot{\epsilon}_2=8x10^{-3}$			$\dot{\epsilon}_3=8x10^{-2}$		
	YS MPa	n -	ϵ_c %	YS MPa	n -	ϵ_c %	YS MPa	n -	ϵ_c %
350	917	.83	no	773	.91	35	-	-	-
500	652	.81	YP	576	.83	9	514	.60	14
575	-	-	-	567	.85	9	-	-	-
650	619	.77	YP	533	.84	4	514	.58	6
700	619	.80	YP	524	.77	4	-	-	-

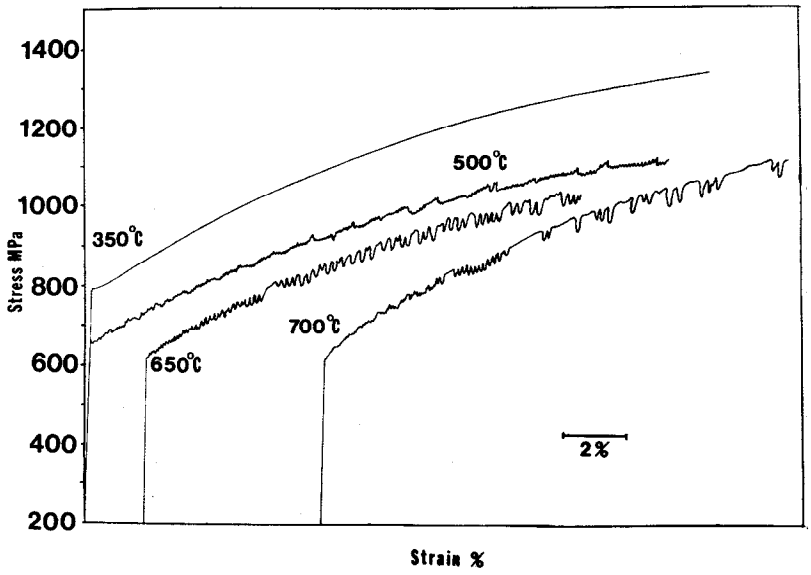

Fig.1. Stress-strain curves in the aged material; strain rate $\dot{\epsilon}_1=8x10^{-4}$.

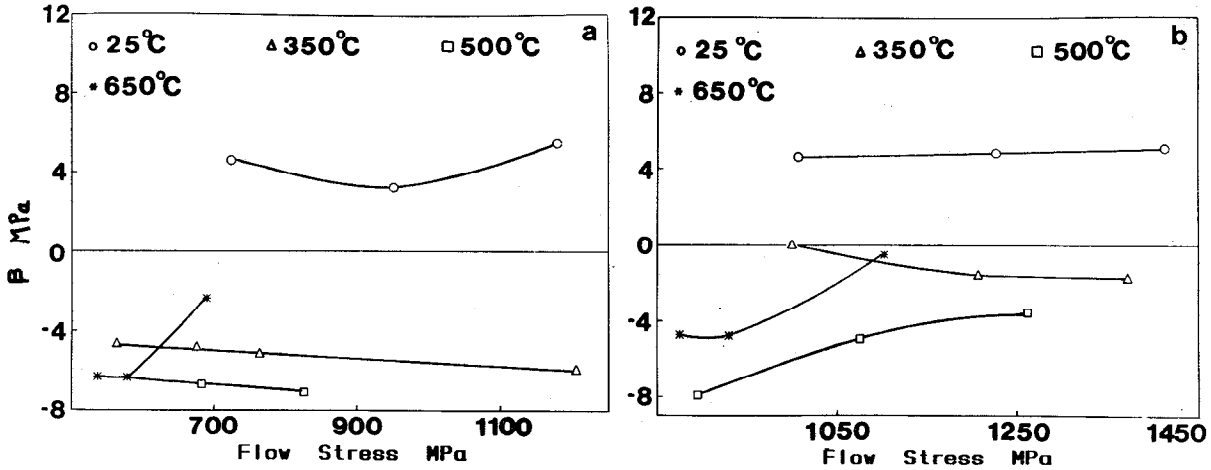

Fig.2. Strain rate sensitivity - flow stress relationships: a) unaged, b) aged material.

Microstructure

Optical and TEM studies of the unaged 242 alloy revealed an essentially single phase material, with an average grain size of about 15 μm and sporadic M_6C carbides.

Typical deformation structure of the unaged specimen deformed at room temperature to 25% is shown in Fig.3. The dislocations form pile-ups and a well-defined banded structure.

After deformation at elevated temperatures, the banded structure became more distinct, the dislocation structure was less uniform, occasionally microtwins occurred, but, by and large, the effect of temperature on deformation structure was not pronounced. The selected area diffraction patterns (SADP) showed typical f.c.c. reflections and diffuse intensity maxima at different positions (1,½,o) coming from short range ordered (SRO) regions (7). Dark field images in the SRO reflections failed to reveal any microdomain structure.

Precipitation of an ordered phase took place during aging. The diffraction patterns of specimens aged at 650°C exhibited extra reflections in addition to the f.c.c. reflections (Fig.4). The extra reflections appear at every ⅓<220>, ⅓<420> and ⅓<311> positions, indicating the presence of a Pt_2Mo-type superlattice (8-10), and the SRO reflections were absent. The dark field image reveals a large volume fraction of uniformly distributed, extremely small ($\approx$10nm), ellipsoidal particles (fig.5). The typical microstructure after $\approx$30% deformation is shown in Fig.6. It is clear that microtwinning became the predominant deformation mechanism in the aged specimens. The microstructure of aged specimens deformed at elevated temperatures was found to be in general very similar to that observed in specimens deformed at room temperature, i.e. it consisted of deformation twins, usually in two systems. The only difference was significant shearing of some deformation twins observed after elevated temperature deformation (Fig.7).

The aging temperature affected the size and shape of the ordered precipitates. In specimens aged above 650°C, coarsening of ordered precipitates was observed, and very thin plate-shaped precipitates were also occasionally noticed. The deformation structure of specimens aged at higher temperatures consisted of dislocation bands as well as deformation twins.

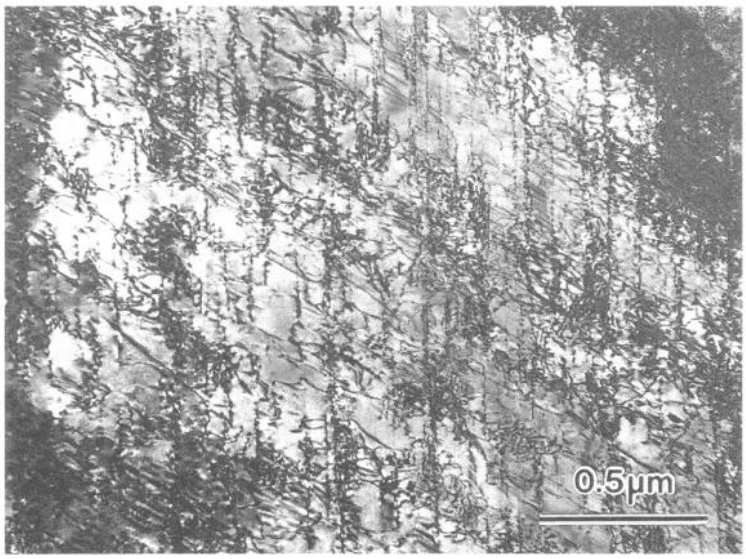

Fig.3. Typical deformation structure of the unaged specimen.

The fracture of unaged and aged specimens occurred by a cup and cone type of rupture. The shear lips were relatively smooth while the central area had a rough, porous appearance. The fractographs taken from the unaged specimens, tested at ambient temperature, indicated that fracture was of the dimple type (Fig.8a). The fracture surface of the aged specimens showed a change in the fracture mode from simple dimple type to a mixture of dimple rupture and cleavage (Fig.8b).

Discussion

Microstructure and Mechanical Properties

The transformation from a disordered to a long range ordered state in the Ni-Mo and Ni-Mo-Cr alloys has been examined in detail by others (7,8,10,11) and is not discussed here. It is well established that the ordering reaction has a continuous character, i.e. LRO domains form from previously nucleated short range clusters or domains. In the present study, the intensity maxima at (1,½,0) positions on diffraction patterns indicate the presence of the SRO domains in the unaged specimens deformed at

elevated temperatures. It is believed the SRO contributes to the retention of strength of the unaged material at 500°C.

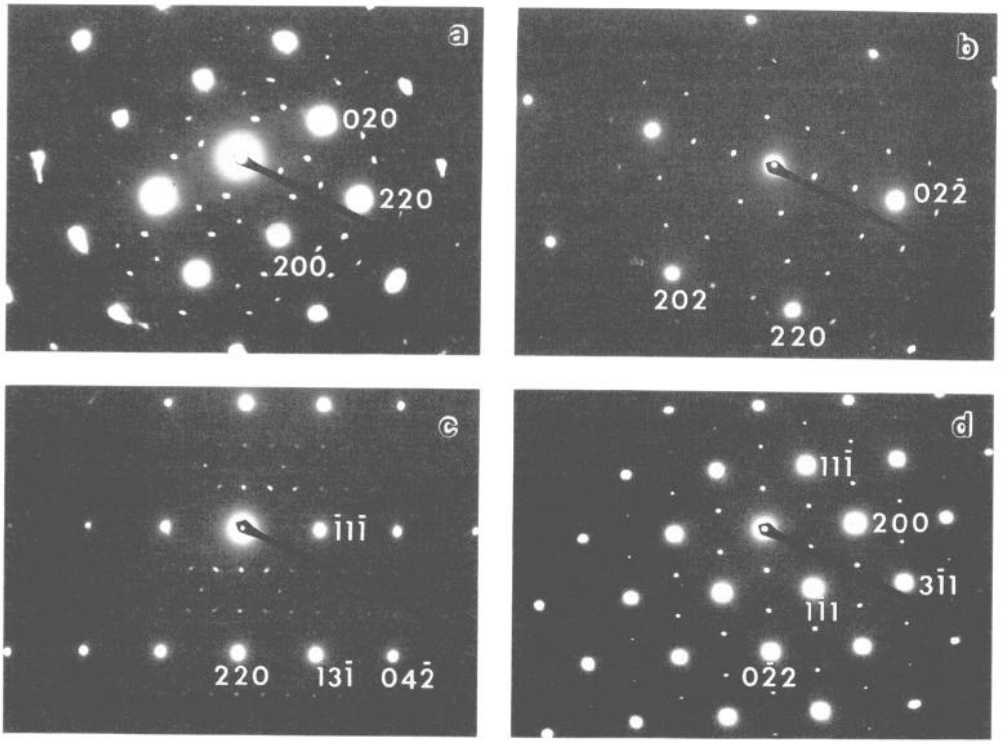

Fig.4. Selected area diffraction patterns from aged specimen:
a) B=[001], b) B=[$\bar{1}$11], c) B=[$\bar{1}$12], d) B=[011].

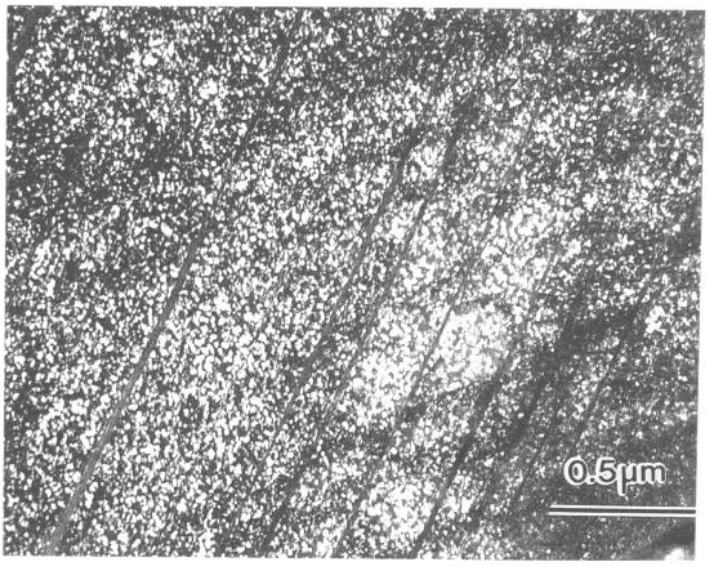

Fig.5. Dark field image of the ordered phase.

A long range ordering reaction leading to the formation of extremely small ($\approx$10nm), Pt_2Mo-type, coherent precipitates occurs during aging at the optimum temperature of 650°C. Characteristic streaking of diffraction spots along <210> directions indicates that the precipitates are plate-like shaped. According to Das et al. (8), such precipitates form as a result of stacking of atoms on either {420} or {220} planes. The Pt_2Mo-type precipitates have been found in many commercial nickel-base alloys containing molybdenum and/or chromium (2,12,13). It is well established that in a binary Ni-Mo system the Ni_2Mo phase is metastable and does not appear in a Ni-Mo equilibrium diagram (9). In the Ni-Cr system, on the other hand, the Ni_2Cr is stable up to about 590°C (14). Since the ternary Ni-Mo-Cr phase diagrams are not available at below 700°C and the quantitative chemical analysis of the ordered phase would be very difficult or even impossible because of the extremely small size of precipitates, one may only speculate that the ordered phase in the 242 alloy has the form of $Ni_2(MoCr)$. This speculation, however, is supported by previous studies on Ni_4Mo-Cr alloys (15) which showed that Cr atoms substitute for Mo

atoms in all observed ordered phases, including Ni_2Mo. Furthermore, chromium can be regarded as an agent stabilizing the metastable Ni_2Mo phase.

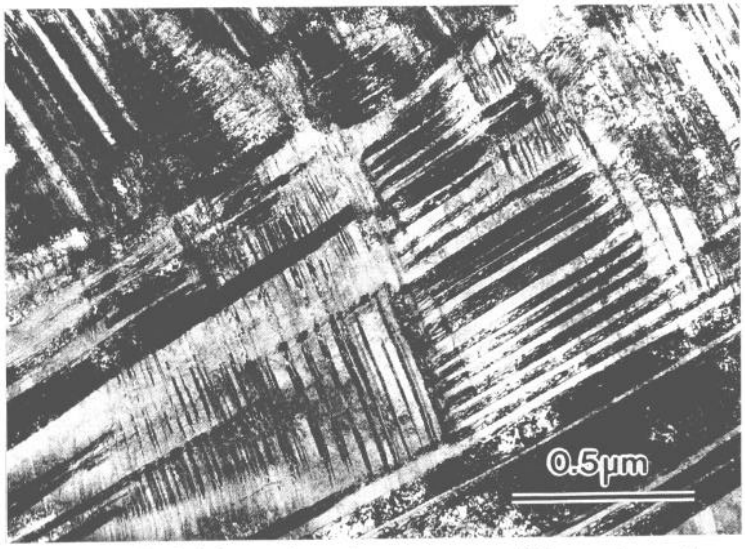

Fig.6. Typical deformation microstructure of the aged specimen ($\epsilon \approx 30\%$).

Due to the presence of the ordered precipitates, the strength of aged specimens is twice that exhibited by unaged ones. The strengthening was accompanied by the striking change in the deformation mode from crystallographic slip to microtwinning. Such a change due to the presence of small ordered particles was reported earlier in: HASTELLOY alloys S, C-4, C-276 (Pt_2Mo-type)(2); Ni-28%Mo alloy (Ni_4Mo)(12); INCONEL®[3] 718 (DO_{22} type) (16). All these phases are crystallographically related and can be derived from the f.c.c. lattice by atomic rearrangements on the {420} planes (17).

The phenomenon of changing deformation mode from slip to twinning was first attributed to the hypothetical lowering of stacking fault energy (SFE) (12). Molybdenum is known to decrease the SFE of Ni-base alloys (18) and chromium is supposed to act in the opposite direction. However, the precipitation of Ni_4Mo ordered phase in a binary Ni-19 at.% Mo alloy did lead to the change in deformation mode from slip to twinning (12), although the content of Mo in the matrix did not change considerably during precipitation, and the SFE of the matrix did not decrease. A semi-quantitative analysis of the present results also does not support the notion that the decreasing SFE of the matrix during ordering is the major factor encouraging the change of deformation mode.

The change of deformation mode has been also discussed in the literature in terms of the effect of the structural change (f.c.c. → orthorhombic) associated with ordering. It was shown that while such a change makes ten of the potential twelve f.c.c. slip systems energetically unfavorable, it makes only two of twelve twining systems unfavorable (19). Moreover, ordered particles constitute strong obstacles for mobile dislocations and are known to restrict cross slip (20).

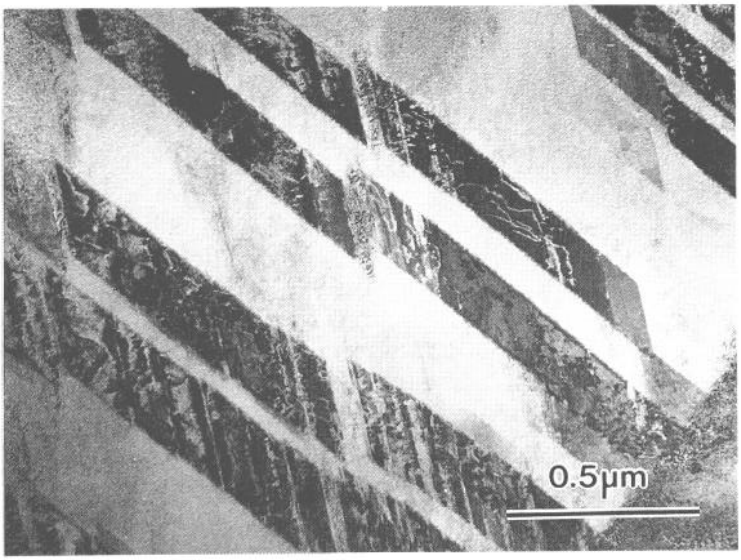

Fig.7. Typical TEM microstructure after elevated temperature (700°C) deformation of the aged specimen.

In the light of the above discussion and the results of our TEM studies, we postulate that in the present aged alloy slip occurs only in the early stages of plastic deformation. After a few % elongation, dislocation pile-ups on the slip planes cause the internal stresses to increase, dislocations cannot change their slip planes (cross-slip is restricted) and the activation of other slip systems is

[3] ® INCONEL is a registered trademark of the Inco Family of companies.

unlikely. As a result, the alloy work hardens very strongly and the stress becomes high enough to activate twinning.

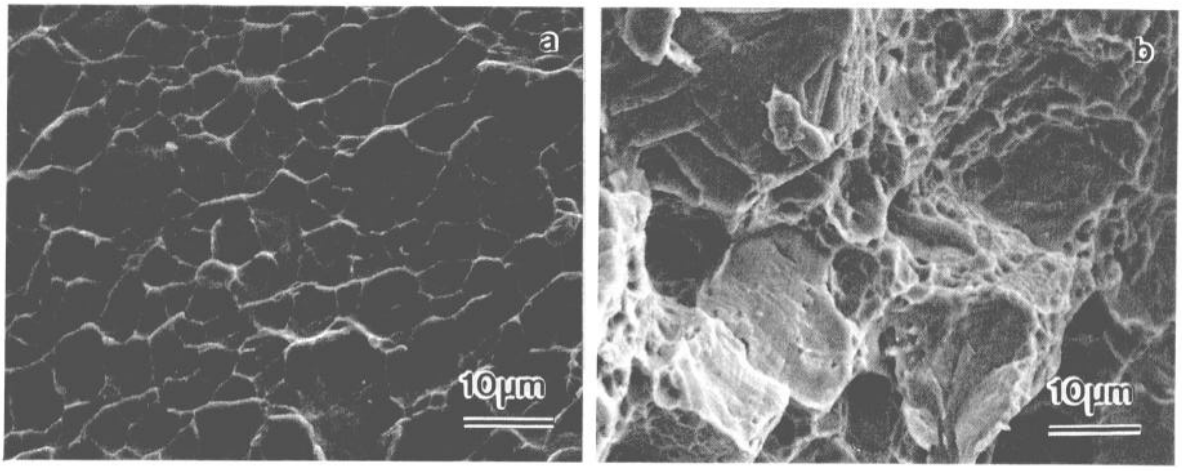

Fig.8. Fracture surfaces of the specimens deformed at room temperature a) unaged, b) aged material

Jerky Flow

Discontinuous deformation, or the so called Portevin - Le Chatelier (P-L) effect (21), manifesting itself as serrated (jerky) flow during tensile tests at elevated temperatures, has been known for almost 70 years, but there are still some discrepancies concerning its origin and explanation.

In the present study, serrations in the stress-strain curves were observed in both unaged and aged specimens. Comparing the results shown in Tables III,IV and Figs. 2a, 2b, one can note that the jerky flow occurred when strain rate sensitivity was negative. This implies that the jerky flow is caused by dynamic strain aging (DSA) (6,22), resulting from the interactions between moving dislocations and diffusing interstitial atoms. On the other hand, the parameter β became negative at temperatures and strains lower than that critical for the appearance of the jerky flow (e.g. aged specimens tested at 350°C) indicating that the mechanism of DSA operated over a wider range of temperatures and strains. The occurrence of the jerky flow was accompanied by strong work hardening. Dynamic strain aging also causes the yield strength to decrease with increasing strain rate. The above results agree well with the results of other studies (22,23), and their general interpretation in terms of dislocation-solute atoms interactions is universally agreed upon (5,6,22-26). There is no consensus, though, as to the details of the mechanism of DSA and the discussion of the present results, especially the differences between the unaged and aged specimens and the role of twinning, is hoped to contribute to improved understanding of the DSA and its manifestation - serrated flow.

In 242 alloy at a given strain rate, the jerky flow appeared in the aged material at higher temperatures and strains. A possible explanations of the delay of jerky flow in aged material may be derived from the classical Cottrell's concept (27). Cottrell assumed that vacancies produced during deformation enhance diffusion of solutes forming atmospheres at dislocations and that alternate atmosphere pinning and breakingaway leads to serrated yielding. In our case, since the creation of vacancies takes place during motion and the interaction of dislocations, aged specimens deformed predominantly by twinning should exhibit lower vacancy concentration than the unaged specimens deformed only by slip. Theoretically predicted (28), experimentally confirmed (29) less rapid diffusion of interstitials in the ordered state may also contribute to the delay.

On the other hand, one could claim that the delay is caused by a lower concentration of carbon in the matrix of the aged material due to carbides formed during aging. However, optical and TEM investigations did not reveal distinct differences in the distribution and morphology of carbides in the unaged and aged materials. To further explore a possible effect of lowering carbon content on serrated yielding, two unaged specimens were annealed at 800°C (a temperature high enough to prevent precipitation of ordered phase) for 9 hours and deformed at 350°C and 500°C. The annealing did not affect the appearance of the resultant stress - strain curves. Therefore the alternative scenario can be

rejected.

In the unaged specimens, one might postulate that "SRO locking" rather then "solute locking" of dislocations is more likely. Sumino (30) calculated the effect of the stress field of a dislocation on the SRO in its vicinity and showed that the ordering effectively locks dislocations. In addition, one might argue that the early onset of the jerky flow at the low strain rate (see Table III) is associated with the SRO as well, because no "waiting time" is needed to lock a dislocation in this case. However, we reject this explanation since the jerky flow and its early initiation were also observed in the aged specimens in the absence of the SRO.

The role of twinning on the character of the stress-strain curves needs to be readdressed. In the aged specimen, dislocations are strongly locked by the dispersed LRO phase and deformation proceeds by twinning. Twinning itself is not likely to produce serrations because it occurs in a random way in the entire volume of a deformed specimen, whereas plastic instabilities leading to serrated flow require large local stress concentrations typically caused by the localized activation of a large number of dislocations (31). In fact, TEM studies indicate that the contribution of slip in the aged specimens increases with increasing temperature.

The occurrence and the extent of the jerky flow in the present alloy differs from the typical characteristics of the jerky flow in other F.C.C. materials. It occurs at higher temperatures (e.g. in Ni-C alloys the jerky flow was reported between -50 - +300°C (32)) and persists till failure (e.g. in INCONEL alloy 600 the jerky flow -occurring at temperatures comparable to these in the present alloy- was observed to be confined to only a few serrations at the very early stages of plastic deformation (22)). Moreover, the character of the instabilities in stress-strain curves changes with increasing strain, the load drops become less frequent and deeper, especially in the aged specimens deformed at 650 and 700°C, and they are accompanied by distinct audible sounds. TEM of the failed aged specimens showed very inhomogeneous deformation leading to apparent shearing of twin boundaries (Fig.7). The reasons for this distinct behavior as well as the diversity of serrations encountered are unclear and being explored. Also, the temperatures at which jerky flow occurs in the present alloy are high enough (0.4-0.6 T_M) for the diffusion of substitutional atoms (Mo) which may contribute to the discussed irregularities in the stress-strain curves.

Conclusions

1. Short range ordering contributes to the retention of strength of the unaged 242 alloy at 500°C.
2. Aging at 650°C for 24 hours results in an optimum combination of mechanical properties. The yield strength of the material doubles compared to that of the unaged material due to the presence of small ordered particles.
3. The deformation mechanism changes from crystallographic slip in the unaged condition to microtwinning in the aged condition. This change is attributed to the presence of the ordered particles which constitute effective dislocation barriers and restrict cross-slip.
4. Characteristic serrations in the stress-strain curves were observed in the unaged and aged specimens deformed at elevated temperatures. The occurrence of the jerky flow coincides with the negative value of strain rate sensitivity, implying a role of dynamic strain aging.
5. The jerky flow was delayed to higher strains and temperatures in the aged specimens, likely due to limited vacancy generation and decreased diffusivities of interstitial atoms.

Acknowledgements

The support of the Haynes International, Inc. is greatly appreciated.

References

1. S.K. Srivastava and G.Y. Lai, "A New Low-Thermal-Expansion, High-Strength Alloy for Gas Turbines", The American Society of Mechanical Engineers, 89-GT-329.

2. H.M. Tawancy, "Long-term ageing characteristics of some commercial nickel-chromium-molybdenum alloys", *J. Mat. Sci.* 16 (1981), 2883.
3. M.F. Rothman, Haynes Int., Technical Information, 1989.
4. S.K. Srivastava and M.F. Rothman, "An Advanced Ni-Mo-Cr alloy for Gas Turbines", Proc. of Int. Conf. on High Temperature Materials for Power Engineering, Liege, Belgium, 1990.
5. A. Van Den Beukel, "Theory of the Effect of Dynamic Strain Aging on Mechanical Properties", *phys. stat. sol.* 30 (1975), 197.
6. P. Wycliffe, U.F. Kocks and J.D. Embury, "On Dynamic and Static Ageing in Substitutional and Interstitial Alloys", *Scripta Met.* 14 (1980), 1349.
7. G. Van Tendeloo, "Short Range Consideration and Development of Long Range Order in Different Ni-Mo Alloys", *Mat. Sci. Eng.* 26 (1976), 209.
8. S.K. Das and G. Thomas, "The Metastable Phase Ni_2Mo and the Initial Stages of ordering in Ni-Mo Alloys", *phys. stat. sol.* 21A (1974), 177.
9. C.R. Brooks, J.E. Spruiell and E.F. Stansbury, "Physical Metallurgy of Nickel-Molybdenum Alloys", *Int. Mat. Rev.* 29 (1984), 210.
10. M. Kumar and V.K. Vasudevan, "Short-Range Ordering Reactions in a Ni-25Mo-8Cr Alloy", *Mat. Res. Soc. Symp. Proc.* vol. 213 (1991), 187.
11. N.S. Mishra and S. Ranganathan, "Electron Microscopy and Diffraction of Ordering in a Ni-25wt.%Mo Alloy", *Mat. Sci. Eng.* 150A (1992), 75.
12. H.M. Tawancy and Abbas, "Effect of Long-Range Ordering on the Corrosion Properties of an Ni-Mo Alloy", *J. Mat. Sci.* 24 (1989), 1845.
13. K. Miyata and M. Igarashi, "Effect of Ordering on Susceptibility to Hydrogen Embrittlement of a Ni-Base Superalloy", *Metall. Trans.* 23A (1992), 953.
14. P. Nash, "The Cr-Ni System", *Bulletin of alloy phase diagrams*, 7 (1986), 466.
15. K. Vasudevan and E.E. Stansbury, *Mat. Res. Symp. Proc.* vol. 62 (1986), 337.
16. M. Sundararaman, P. Mukhopadhyay and S. Banerjee, *Acta Met.* 36 (1988), 847.
17. H.M. Tawancy and M.O. Aboelfotoh, *phys. stat. sol.* 99 (1987), 461.
18. T.C. Tiearney and N.J. Grant, *Metall. Trans.* 13A (1982), 1827.
19. P.D. Johnson, PhD thesis, University of Notre Dame, Indiana, 1980 (after Ref. (2)).
20. V. Gerold and H.P. Karnthaler, "On the Origin of Planar Slip in F.C.C. Alloys", *Acta Met.* 37 (1989), 2177.
21. L.J. Cuddy and W.C. Leslie, "Some Aspects of Serrated Yielding in Substitutional Solid Solutions of Iron", *Acta Met.* 20 (1972), 1157.
22. R.A. Mulford and U.F. Kocks, "New Observations on the Mechanisms of Dynamic Strain Aging and of Jerky Flow", *Acta Met.* 27 (1979), 1125.
23. T.A. Bloom, U.F. Kocks and P. Nash, "Deformation Behavior of Ni-Mo Alloys", *Acta Met.* 33 (1985), 265.
24. A. Van Den Beukel, "On the Mechanism of Serrated Yielding and Dynamic Strain Aging", *Acta Met.* 28 (1980), 965.
25. P.G. McCormick, "Theory of Flow Localization Due To Dynamic Strain Aging", *Acta Met.* 36 (1988), 3061.
26. L.P. Kubin and Y. Estrin, "Evolution of Dislocation Densities and the Critical Conditions for the Portevin-Le Chatelier Effect", *Acta Met.* 38 (1990), 697.
27. A.H. Cottrell, *Phil. Mag.* 44 (1953), 829.
28. M.A. Krivoglas and A.A. Smirnov, "The Theory of Order-Disorder in Alloys", Macdonald (1964).
29. F.M.C. Besag and R.E. Smallman, "Discontinuous Yielding in Ordering Alloys", *Acta Met.* 18 (1970), 429).
30. K. Sumino, *Sci. Rep. Res. Inst.* Tohohu Univ. I.A.J. 10 (1958), 283 (after Ref. (29)).
31. A. Korbel, J. Zasadziński and Z. Sieklucka, "A New Approach to the Portevin-Le Chatelier Effect", *Acta Met.* 24 (1976), 919.
32. U.F. Kocks, R.E. Cook and R.A. Mulford, "Strain Aging and Strain Hardening in Ni-C Alloys", *Acta Met.* 33 (1985), 623.